Modelling and process analysis of hybrid hydration-absorption column for ethylene recovery from refinery dry gas

Xiaobo Luo[a], Meihong Wang[a,*], Xingang Li[b,c,*], You Li[b], Chao Chen[b], Hong Sui[b,c],

[a] *Process and Energy Systems Engineering Group, School of Engineering, University of Hull, HU6 7RX, UK*

[b] *School of Chemical Engineering and Technology, Tianjin University, Tianjin 300072, China*

[c] *Collaborative Innovation Center of Chemical Science and Engineering (Tianjin), Tianjin 300072, China*

**Corresponding author 1: Email:* Meihong.Wang@hull.ac.uk

**Corresponding author 2. Email:* lxg@tju.edu.cn

Abstract:

Effective recovery of ethylene from dry gas plays an increasingly important role to improve economic performance of refineries. Conventional approaches such as cryogenic separation and cold oil absorption are energy consuming. Hybrid hydration-absorption (HHA) process may be an effective way as hydrate formation takes place at temperature near the icing point. This paper aims to study the HHA column, which is the heart of the HHA process, through modelling and process analysis. A detailed steady state model was developed in gPROMS® for this vapour-liquid-water-hydrate (V-L-W-H) four phases system. A base case was analysed with real industry data as inputs. The composition distribution profiles inside the column were explored and the key parameters related with kinetics-controlled hydration process were investigated. Three case studies were carried out for different C_2H_4 concentrations in gas feed, L/G ratios and temperature profiles respectively. The results show (a) the separation performance of CH_4 and C_2H_4 in the HHA process remains significant for big range of C_2H_4 feed concentration; (b) L/G ratio has a great impact for hydrate formation and the separation performance of CH_4 and C_2H_4 improves when L/G ratio increases until reaching an optimal point; and (c) a cooling system is required to draw out the heat generated inside the HHA column so that the operating temperature of each plate can be at the temperature near the icing point to retain hydrate formation. This study indicates that the HHA process may be a more promising approach to recover ethylene from refinery dry gas in future industry application.

Keywords: Ethylene Recovery, Refinery Dry Gas, Hydration, Process Modelling, Process Design and Operation

1. Introduction

1.1 Background

Ethylene is an important basic raw material in petrochemical industry. Oil refineries produce a large amount of dry gas with high ethylene content, such as delay coking gas and fluid catalytic cracking (FCC) gas [1]. Thus recovery and reuse of ethylene from oil refinery dry gases are important to improve the plant economic profile especially in the case oil refineries produce more light olefins nowadays [2]. Refinery dry gases mainly contain typical low boiling gas mixtures such as CH_4, C_2H_4, C_2H_6, N_2, H_2 [1]. The conventional technologies for separating this low boiling gas mixture are cryogenic separation and cold oil absorption. The separation process of this light gas mixture requires a huge amount of energy. For example, cryogenic distillation approach employs an energy consuming refrigeration process [3]. For oil absorption, large solvent cycle rate is required for high recovery rate, which makes both larger size of equipment and high regeneration energy. Some other technologies, such as solvent extraction, chemical absorption, pressure swing adsorption and membrane separation were also studied [3], but their industry application are not common.

A novel method is to use clathrate hydrate [4] to separate ethylene and ethane from refinery dry gas. An advantage of hydrate approach over cryogenic separation is that hydrate formation can take place at the temperature around the icing point, thus deep cooling could be avoided. However two disadvantages, slow hydration rate and agglomeration, were also observed, which make it hard to combine hydration process into continuous operation process. Recent studies found water-in-oil emulsion introduced into hydrate formation process could not only enhance the hydrate formation rate and improve single stage separation efficiency but also prevent the hydrate agglomeration [5]. With this finding, the process of combining the oil absorption process and hydration process [6] was designed to recover ethylene and ethane from oil refinery dry gas.

1.2 Previous researches

Gas hydrate (also known as clathrate hydrate) is water-based solids with physical properties resembling ice, in which small guest molecules, such as low molecular weight gases methane as well as some light hydrocarbons and freons, are trapped in cages of hydrogen bonded host water molecules [4]. Three types of hydrate structures have been determined: sI, sII, and sH depending upon the temperatures and pressures of formation processes and the compositions if a gas mixture was involved [7]. Gas hydrate attracted the research intention as one of main problems in the gas transportation from 1934 [8]. Later wide distribution and huge capacity of natural gas hydrates are found in deep water all over the world, which could be a source of future fuel [9]. A novel application of gas hydrate is the separation of gas mixture [10], such as separation of C_2H_4 from CH_4 + C_2H_4 mixture and other components like CO_2, CH_4 and H_2S. By managing temperatures and pressures of hydrate formation processes, hydrate may exhibit different selectivity to different gas components in a gas mixture. Meanwhile, weak hydrogen bonds of hydrate are easy to be broken with a little energy requirement, which makes it easy to enrich objective gas and to circulate the solvent by regenerating the rich solvent.

Recent fundamental studies focus on the thermodynamics of hydrate and kinetics of its formation and dissociation. Van der Waals and Platteeuw [11] proposed a statistic thermodynamics model for the phase equilibrium in porous media, which was used with Gibbs-Thomson relationship to determine the interfacial tension between hydrate and water from experimental data. Later a thermodynamics model based on the concepts of reaction and adsorption two-step formation mechanism was reported by Chen and Guo [12-13]. The study of the kinetics of hydrate formation is hard because the process happens in pores are difficult to control and monitor [14]. Englezos et al. [15] observed that the formation rate is a strong function of the driving force and that formation occurs in both the interface and the liquid phase. The kinetic model proposed by Kashchiev and Firoozabadi [16] expresses the driving force is the supersaturation chemical potential difference, which depends on the actual gas concentration in the solution. Thus the particular conditions of gas dissolution into the aqueous phase have significant impact on the hydrate formation rate. Later Genanenderan and Amin [17] extended Kashchiev-Firoozabadi model for hydrates formation in spray reactors and gained the satisfactory results compare to experimental data.

For using hydrate formation to separate ethylene and ethane from refinery dry gas, low formation rate and agglomeration were observed, which make it hard to integrate hydrate process into the continual process in industry scale. Ma et al. [5] conducted experimental studies on the hydrate equilibrium and formation kinetics for a simulated catalytic cracking gas in the water-in-oil emulsion. The study demonstrates that gas hydrate formation rate can increase enormously and hydrates agglomeration would mitigate in the water-in-oil emulsion compared with in pure water. The results showed that hydrogen and methane can be separated from the C2+ component by forming hydrate at around 273.15 K at the pressure ranging from 3.5 to 5 MPa. In their later study [18], the phase equilibrium of vapour–liquid–water–hydrate multiphase was studied. The Patel–Teja (PT) equation of state (EOS) was used to perform the vapour–liquid–liquid three-phase flash calculation and the Chen–Guo two-step hydrate model was employed to calculate the vapour–hydrate phase equilibrium. This method is rather simple in order to avoid the complexity of simultaneous solution of the sophisticated equation group.

However the modelling of HHA process stays on an early stage and relies on a relatively simply level. The only one related model was developed by Ma and Chen [19]. They developed a model of hydration-absorption column in water-in-oil emulsion with kinetics-controlled hydration process and equilibrium absorption process. But their model assumed 500 stages of finite elements then it neglects the impact of realistic column internals to some key parameters related with the kinetics-controlled hydration process. Their model did not include the water phase so that it could not make energy conservation calculation. Thus the model simply calculates the heat generated from hydration process without considering the absorption heat and the temperature of each stage is fixed by assuming all heat is drawn out from each stage. Those shortcomings may bring big uncertainties when the model is used to do the process analysis or to guide the designs of pilot plant. Therefore, more research efforts are required in the advanced modelling of HHA process in order to provide an effective method and tool for both technical and economic assessment for further studies and potential industry application.

1.3 Aim and novel contributions

The aim of this study is to explore HHA column through modelling and process analysis to gain insights for further whole HHA process analysis in the context of ethylene recovery from refinery dry gases. Serving this aim, there are two objectives which are defined as follows: (1) to develop a steady state first principle model of HHA column and to implement in gPROMS® and (2) to perform process analysis of HHA column by conducting simulations using the model developed.

Compared with the study published by Ma and Chen [19], there are three novelties in this study: (1) the selection of column type was discussed qualitatively. The finding is that plate column is more suitable for HHA column compared with packed column; (2) a detailed first principle steady state model was developed and implemented in gPROMS® based on a sieve plate column. The model includes V-L-W-H four phase system and mass and energy conversation, which provides an accurate prediction of HHA process; and (3) process analysis was carried out for the base case with a real FCC dry gas data as inputs and three case studies were conducted for different C_2H_4 concentrations in gas feed, L/G ratios and temperature profiles inside the column. The results indicate that HHA process may be a better approach to recover ethylene from refinery dry gas in future industry application.

2. HHA process and column equipment

2.1 HHA process

With the advantage of less energy requirement, hydrate separation is expected to be used to recover ethylene from refinery dry gas [20]. In one recent patent [6], the hydration process was considered to integrate with conventional oil absorption process for the application of ethylene recovery from FCC dry gas or ethylene gas.

In this HHA process shown in Fig.1, FCC dry gas or ethylene gas is pressurized to a high pressure of 2.0-4.0Mpa, and then enters an HHA column with hydrous slurry feeding at the top. The operating temperature and pressure of the HHA column were 263.15-283.15K and 2.0-4.0Mpa respectively. C2 components enrich in the slurry bottoms because of absorption and hydration and are discharged into the hydrate dissociation tank. The gas-depleted overhead, still with a low content of C2 components, enters the hydration reactor with an operating pressure of 2.0-4.0Mpa, in which low content C2 components continue to form hydrate to increase the recovery rate. With minor heat requirement for increasing the temperature of the tank, C2 components are released by hydrate dissociation. A part of the C2 components goes back to the HHA column for stripping, which could help improve the mole fraction of C2 components in hydrate phase. Another part of C2 components goes to the ethylene tower directly or via further purification unit depending on the impurities content. The slurry bottoms of the tank were recalculated to the hydration reactor after resolving, cooling and pressurization. This HHA process was expected to have a low energy cost to achieve an effective recovery of ethylene and ethane with both high recovery rate and high purity.

2.2 Column type selection for HHA process

In conventional cold oil absorption (COA) process, the absorber could be a plate column or a packed column. But the operational conditions of the column in HHA process are different with COA absorber. Compared with conventional COA absorber, the operating pressure of HHA column is significantly higher to satisfy the hydrate formation conditions

[4]. At the same time, hydrate solids will be formed in the oil liquid phase, which make it easy to block the equipment in narrow flow path. More importantly, the hydrate formation rate is slow although water-in-oil emulsion accelerates the hydrate formation, which requires longer liquid residence time to ensure the total amount of hydrate formation. The comparison results (see Table 1) show plate column has better adaptabilities than packed column for HHA column. Thus plate column was chosen for the HHA column in this study. Additionally, sieve plate was used for the detailed hydraulic calculation because sieve plate has a simple plate structure, which make it has a good resistance for plug risk.

3. Model development for the HHA column

The HHA column is a key equipment of whole HHA process and its modelling is one of the major challenges because V-L-W-H four phases are involved in this multi-stage column. In this section, a detailed steady state model for the HHA column was developed based on sieve plates column. Thermodynamic properties of the vapour-liquid-water (V-L-W) phases were obtained using Peng-Robinson (PR) EOS [23] and Chen-Guo method [12-13] was used for vapour-hydrate phases. The model presented in this study was implemented in gPROMS®.

3.1 Model assumptions

The model developed in this work is improved from the published model by Ma and Chen [19]. As illustrated in Fig.2, a plate column is represented as a cascade of stage for this V-L-W-H system. The equations used to describe this plate column include mass and energy conservation, equilibrium for V-L-W phases and kinetics controlled hydrate formation. The following assumptions were made in modelling this plate column:

- The mixture on each plate is assumed to be well-mixed.
- Two steps, absorption and hydration, are assumed to take place on each stage;
- For absorption, phase equilibrium prevails at the V-L-W mixture.
- For hydration, ’reactions’ are assumed to be kinetics controlled.
- Negligible hydrate dissociation (i.e. breakdown) is assumed.
- Negligible heat loss from the wall of the column is assumed.

3.2 The conservation equations

For the steady state model, there is no material accumulated on the stage. Total material balance for component *i* on plate *j*, taken on a molar basis is given by:

$$V_{j+1}y_{i,j+1}+L_{j-1}x_{i,j-1}+W_{j-1}z_{i,j-1}+HY_{j+1}m_{i,j+1} = V_jy_{i,j}+L_jx_{i,j}+W_jz_{i,j}+HY_jm_{i,j} \qquad (1)$$

For number 1 and number N stages, the vapour feed and solvent feed should replace corresponding streams.

When vapour and liquid enter the stages, V-L-W equilibrium flash is assumed to happen first, thus the mass balance equations are like below:

$$V_{j+1}y_{i,j+1} + L_{j-1}x_{i,j-1} + W_{j-1}z_{i,j-1} = V^f{}_j y^f{}_{i,j} + L_j x_{i,j} + W_j z_{i,j} \tag{2}$$

Then hydration happens as a second step, the mass balance equations are

$$V^f{}_j y^f{}_{i,j} - HG_j = V_j y_{i,j} \tag{3}$$

Mole fractions in the streams leaving each plate must sum to unity, as below equation.

$$\sum_{i=1}^{C} x_{j,i} = \sum_{i=1}^{C} y_{j,i} = \sum_{i=1}^{C} y^f{}_{j,i} = \sum_{i=1}^{C} z_{j,i} = \sum_{i=1}^{C} m_{j,i} = 1 \tag{4}$$

Energy conservation equations are

$$\begin{aligned} &H_{V,j+1} + H_{L,j-1} + H_{W,j-1} + H_{HY,j-1} + H_{abs,j} + H_{hyd,j} \\ &\qquad = H_{V,j} + H_{L,j} + H_{W,j} + H_{HY,j-1} + Q_j \end{aligned} \tag{5}$$

The heat of hydration of each component can use the experimental data for each component respectively. Their value can be seen in Table 2.

3.3 The Kinetics controlled hydration

The total hydrate generated on each stage can be calculated by equation (6):

$$HG_j = r_j \Delta t_j SP_{,j} \tag{6}$$

The hydrate generation rate can be calculated based on the kinetic controlled model proposed by Kashvhiev and Firoozabadi [20]. As the original model was proposed based on the experiments of stirring tank with pure water system, some modifications are required before it is used for plate column in water-in-oil emulsion system. The modified equation was presented by Ma and Chen [19], as below:

$$r_j = K_D K \frac{R_e^{1.64}}{R_{ec}} \left(\frac{P}{P_0}\right)^a \left(\frac{T_0}{T}\right)^b \left(e^{-\frac{\Delta\mu}{RT}} - 1\right)^n \times exp\left[-\frac{1}{RT}\left(\Delta\mu + \frac{R_e{}^{-0.28}\varphi^3 A}{\Delta\mu^2}\right)\right] \tag{7}$$

In this equation, some parameters were obtained from the experiments [19]. $K_D = 0.00042$, $a = 1.53$, $b = 19.7$, $\varphi = 0.118$, $n = 0.5$. K and A can be calculated by below mixing principles. The values of K_i and A_i can be seen in Table 2.

$$K_j = \sum x_{j,i}^{*} K_i \tag{8}$$

$$A_j = \sum x_{j,i}^{*} A_i \tag{9}$$

The driving forces are the differences of Gibbs free energies between vapour and hydrate phases. In Chen-Guo model, it can be calculated by the following equation:

$$\Delta\mu_j = RT_j \left[\lambda_1 ln\left(1 - \sum_i \theta_{j,i}\right) + \lambda_2 \sum x_{j,i}^{*}\, ln \frac{f_{j,i}^{0}}{f_{j,i}}\right] \tag{10}$$

3.4 The thermodynamic model for hydration

Chen-Guo equations calculate the adsorption of hydrocarbon in small and large hydrate holes separately [16-17]. The values of parameters can be seen in Table 3 and Table 4.

For small cages,

$$\theta_{j,i} = \frac{f_{j,i}^{V} C_{j,i}}{1+\sum_j f_{j,i}^{V} C_{j,i}} \tag{11}$$

$$C_{j,i} = X_i \cdot exp\left(\frac{Y_i}{T_j - Z_i}\right) \tag{12}$$

For large cages,

$$m_{j,i}^{*} = \frac{f_{j,i}^{V}}{f_{j,i}^{0}\left(1+\sum_j \theta_{j,i}\right)^{\alpha}} \tag{13}$$

$${f_{j,i}}^{0} = {f_{Tj,i}}^{0} \cdot exp\left(\frac{\beta P_j}{T_j}\right) \alpha_{w,j}^{-1/\lambda_2} \tag{14}$$

$${f_{T,j,i}}^{0} = exp\left(\frac{-\sum_j A_{ij}\theta_{j,i}}{T_j}\right) \cdot \left[{A_i}' exp\left(\frac{{B_i}'}{T_j - {C_i}'}\right)\right] \tag{15}$$

$$m_{j,i} = \frac{{m_{j,i}}^{*} + \alpha\theta_{j,i}}{\sum_{i=1}^{c}\left({m_{j,i}}^{*} + \alpha\theta_{j,i}\right)} \tag{16}$$

$$\alpha = \lambda_1/\lambda_2 \tag{17}$$

3.5 The hydraulic model

The hydraulic calculations for a sieve plate column refer to the book edited by Sinnott [22]. The pressure drops are assumed to be given:

$$\Delta P_j = 9.81 h_{tj} \rho_{Lj} \tag{18}$$

$$h_{tj} = h_{dj} + (h_{wj} + h_{owj}) + h_{rj} \tag{19}$$

$$h_{dj} = 51 \left[\frac{\mu_{bj}}{C_0}\right]^2 \frac{\rho_{Vj}}{\rho_{Lj}} \tag{20}$$

$$h_{rj} = \frac{12.5\times10^3}{\rho_{Lj}} \tag{21}$$

$$h_{owj} = 750 \left[\frac{L_{wj}}{\rho_{Lj} l_{wj}}\right]^{2/3} \tag{22}$$

The residence time of each plate can be calculated based on the liquid volume on the sieve plates and in downcomers. The equations are

$$\Delta t_j = \frac{L_j}{\rho_{Lj}\left[(h_{wj}+h_{owj})\frac{\pi}{4}D^2+(h_{tj}+h_{dcj})0.3166D^2\right]} \tag{23}$$

$$h_{dcj} = 166 \left[\frac{L_{wj}}{\rho_{Lj} A_{mj}}\right]^2 \tag{24}$$

3.6 The hydrate structure

In the presence of small guest molecules, for example its application for low boiling gas mixture separation, hydrate exists in two different structures commonly: structure I (SI) and structure II (SII). For pure gas, its hydrate structure can be confirmed depending on the hydration temperature and pressure. For the gas mixture, the concentrations of each component should be considered. Ballard and Sloan Jr [25] reported phase behaviours for methane-ethane-water mixture, which is used to decide the hydrate structure in this study. When SI and SII hydrate coexist, the ratio of the two hydrate structures needs to be calculated by equation (25) [26].

$$m_{j,i} = \frac{{n_j}^{\mathrm{I}} m^{\mathrm{I}}_{j,i} + {n_j}^{\mathrm{II}} m^{II}_{j,i}}{{n_j}^{\mathrm{I}} + {n_j}^{\mathrm{II}}} = \frac{m^{\mathrm{I}}_{j,i} + \eta_j m^{II}_{j,i}}{1+\eta_j} \tag{25}$$

Hence, η is the ratio of two hydrate structures can be given by equation (26).

$$\eta_i = \frac{n^{II}}{n^{I}} = \left[exp\left(-a\frac{\Delta G^{II}}{RT}\right) - 1\right] / \left[exp\left(-a\frac{\Delta G^{I}}{RT}\right) - 1\right] \quad (26)$$

4. Process analysis of HHA column

The purity of the C2 product is around 90 mol% using conventional oil absorption to recover C_2H_4 and C_2H_6 from dry gas. The HHA approach is expected to reach same requirements with lower energy consumption. Here HHA approach is an integrated system (see Fig.1) includes the HHA absorber, hydrate reactor, hydrate dissociation tank and other auxiliary equipment. However, the study in this paper focuses on the single HHA column which is hard to be specified with an absorption efficiency or recovery rate requirement separately. In this section, process analyses for the base case and other scenarios were carried out by rating simulations, in which a column with 20 sieve trays was designed, to explore the inscapes of HHA process such as component distributions in different phases, key hydrate kinetics parameters and thermal effects.

4.1 Base case

FCC off-gas consists of mixtures of various gases including H_2, O_2, N_2, CH_4, ethane, ethylene, propane, C4+ heavier components and impurities. A typical FCC off-gas was selected as the feed of the HHA column entering the bottom of the column, whilst the mixture of decane and water (see in Table 5) was selected as the solvent feeding from the top of the column. Considering the fluidization of the mixture (slurry after hydrate solids are formatted during the process) and enough water content for hydrate formation, the water concentration in the solvent is 70% volume. The operating pressure is 3.0Mpa. The operating temperature of each plate is maintained at 274.15K by installing a cooling system for each plate to draw out the heat generated by HHA process.

The model gives a hydraulic calculation to gain some key parameters for the calculation of kinetics-control hydration process. The main parameters of the column hydraulic calculation and its results could be found from Table 6. For HHA process, the considerations of solvent flow rate include (1) providing enough oil content for both fluidization and absorption and (2) enough water for hydrate formation. The L/G ratio is relatively higher than normal absorption process. At the same time, higher residence time of liquid would increase the total hydrate formation rate. The weir height is 0.08 meter and the weir length/diameter ratio is 0.85 for the plate design, which would help to increase the residence time of liquid.

The distributions of major components such as H_2, N_2, CH_4, C_2H_4 and C_2H_6 in different phases inside the column were displayed for the base case in Fig.3. The solubility of C_2H_4 is higher than CH_4 in the oil phase although their concentrations in vapour phase are close. In hydrate phase, the C_2H_4 fraction is about 2 times more than the CH_4 fraction. The reason is that the driving force of C_2H_4 hydration is bigger than CH_4 hydration as the C_2H_4 occupies base caves (big caves) in hydrate.

Fig.4 shows the key parameters of each plate related with the kinetic controlled hydrate formation process. The driving force is high on the top two plates whilst it is relatively low and remains stable on other plates. The reason may be the solvent feed has no hydrate content in this single column simulation, and then the difference of Gibbs free energy between vapour and hydrate on the top plates is larger than on other plates. The hydrate formation rate increases greatly from the top plate to the bottom plate. Its value is sensitive to the turbulence degree of the fluids on the plates. Because of both bigger vapour and liquid flow rate at the bottom plates, the Renaults Number is bigger on the bottom plate than the top plate. As a result, the total vapour consumption increases from the top plates to the bottom plates.

4.2 Case studies

4.2.1 Different C_2H_4 concentrations in gas feed

This case study is to investigate the performance of HHA column when the C_2H_4 concentration varies in gas feed. For the case setting up, the C_2H_4 concentration varies from 10 mol %, 20.54 mol% (same as the base case) and 30 mol%. The N_2 concentration in the gas feed will reduce correspondingly and other components stay the same as in the base case to maintain the same mole flow rate of the gas feed. C_2H_4/CH_4 mole ratio was used to be an indicator for discovering the separation of CH_4 and C_2H_4 inside HHA column. Fig.5 displays the results of C_2H_4/CH_4 mole ratio in different phase and total hydrate formation on the plates. C_2H_4/CH_4 mole ratios in hydrate keep about four times of its value in the vapour phase even when C_2H_4 concentration in gas feed is low, which indicates the separation performance of CH_4 and C_2H_4 of HHA column remains good even at low C_2H_4 concentration. It is noticed that the changes of total hydrate formation per stage is not in proportion with C_2H_4/CH_4 mole ratio because N_2 hydrate formation rate is much lower than C_2H_4.

The results of this case study are consistent with some basic hydrate theories. Because of the size of molecule, CH_4 molecules trend to occupy the small caves first whilst C_2H_4 and C_2H_6 molecules can only occupy the big caves [4]. With this feature, the C2 components molecules avoid the competitions from CH_4 molecules even at the low concentration. Especially, with relatively low CH_4 and C2 components concentration, the mixture forms SI structure hydrate [25], in which the number of big caves is three times of the number of small caves. That is why hydrate formation would be effective and cost-efficient method for the separation of CH_4 and C2 components in gas mixture. Compared with it, conventional cold oil absorption requires a sharply increasing solvent recycle rate when C2 components are in very low concentration in gas mixture, which means it operates at a high solvent material cost and energy cost.

4.2.2 Different L/G ratios

This case study is to explore the performance of HHA column when the L/G ratio varies for a fixed gas feed composition. For the case setting up, the L/G ratio in mole varies from 0.5, 1.0 (same with the base case) and 1.5. Correspondingly the flow rate of the solvent feed (including oil and water) increases obviously at higher L/G ratio scenarios. Fig.6 displayed the results including total flow rate of vapour and hydrate and C_2H_4 mole fraction in vapour and hydrate phase under different L/G ratio. The results show that the total mole flow rate of vapour phase decreases and the total flow rate of hydrate phase increases with the increase of L/G ratio obviously. The C_2H_4 mole fraction decreases in vapour phase which indicate the separation of CH_4 and C_2H_4 become better. It is also noticed that the C_2H_4 mole fraction in hydrate reaches maximum values at L/G ratio of 1.0, after that it drops when L/G ratio increases to 1.5. The reason may be the concentration of other components becomes higher which makes the driving force of C_2H_4 hydration to decrease under higher L/G ratio.

4.2.3 Temperature profile

Both absorption and hydration are exothermic processes. In the base case, a cooling system was assumed to draw out the heat generated by absorption and hydration to maintain the plates at a fixed operating temperature of 274.15K. This case study explores the temperature profile of the column if there is no heat exchange between the column and surroundings. One special assumption should be made for this case study is that the hydrate formation could take place even if the temperature is higher than its dissociation temperature. Fig.7 (a) shows the system could not keep the operating temperature of each plate near the icing point. Especially a big temperature bulge is observed for the bottom plates. The reason is that a large amount of heat generated by the hydrate formation on the bottom plates (see in Fig.7 (b)), on which the hydrate generation rates are higher than on the top plates. Actually at the high temperature, hydrate formation could not take place at all. This result indicates a cooling system should be required to draw out the heat generated inside the column to ensure the performance of HHA process.

5. Conclusions and recommendations for future work

In this paper, the modelling and process analysis of HHA column has been investigated in order to gain insights for further whole HHA process analysis for its application for ethylene recovery from refinery dry gases or ethylene gas. The type selection of HHA column, a key equipment of this hybrid process, was discussed qualitatively. Plate column exhibits several better adaptabilities than packed column. A sieve plate column was chosen to be the physical base for later modelling work. A steady state model was developed in gPROMS® to describe V-L-W-H four phases system in the HHA column. The model uses equilibrium stage for V-L-W phases and kinetics-controlled hydrate formation process. PR EOS was used as the thermodynamics method V-L-W equilibrium and Chen-Guo method was used for hydrate formation.

A base case was simulated with a real FCC gas as the feed. The column was sized in details and the composition distribution inside the column was explored. The key parameters related with rate-based hydrate formation process were discussed. Three case studies were conducted for different C_2H_4 concentration in gas feed, L/G ratio and temperature profiles inside the column. The results show (1) the separation performance of CH_4 and C_2H_4 remains good when the C_2H_4 concentration in gas feed decreases from 30 mol% to 10%, (2) L/G ratio has a big impact for hydrate formation and the separation performance of CH_4 and C_2H_4 becomes better when L/G ratio increases until reaching its optimal point, and (3) a cooling system is required to draw out the heat generated by HHA process to ensure the operating temperature of each plate near the icing point.

As the first step of whole system modelling, the study in this paper obtained some insights of the hydration-absorption process inside a tray column which may guide the design and operation of future pilot plants for validation purpose. However the overall performance such as purity requirement and recovery rate of C2 components was not analysed for the HHA column considering no clear requirement boundaries between this column and whole HHA process. For future studies on a whole HHA system, purity and recovery rate of C2 components could be specified as key performance indexes whilst the economic profile could be evaluated for optimal design and operation of the integrated HHA process.

Acknowledgement

The authors would like to acknowledge the financial support from 2013 China-Europe small-and-medium sized enterprises energy saving and carbon reduction research project (No.SQ2013ZOA100002) and the Basic National Research Program of China (No. 2012CB215005).

References

[1] Parkash S. Refining processes handbook: Gulf Professional Publishing; 2003.

[2] Soni D, RAo MR, SAiDulu G, BhATTAChARyyA D, SATheeSh V. Catalytic cracking process enhances production of olefins. Petroleum Technology Quarterly 2009;4.

[3] Peramanu S, Cox BG, Pruden BB. Economics of hydrogen recovery processes for the purification of hydroprocessor purge and off-gases. International Journal of Hydrogen Energy 1999;24(5):405-424.

[4] Sloan Jr ED, Koh C. Clathrate hydrates of natural gases: CRC press; 2007.

[5] Ma Q, Huang Q, Chen G, Wang X, Sun C, Yang L. Kinetic and Phase Behaviors of Catalytic Cracking Dry Gas Hydrate in Water-in-Oil Emulsion. Chinese Journal of Chemical Engineering 2013;21(3):295-300.

[6] Tianjin University , Inventor device and method for ethylene cracking FCC dry gas or gas ethylene, ethane hydrate absorption stripping for recycling. P.R. China2014 May 7, 2014.

[7] Dendy Sloan E. Clathrate hydrate measurements: microscopic, mesoscopic, and macroscopic. The Journal of Chemical Thermodynamics 2003;35(1):41-53.

[8] Hammerschmidt EG. Formation of Gas Hydrates in Natural Gas Transmission Lines. Industrial & Engineering Chemistry 1934;26(8):851-855.

[9] Makogon YF. Natural gas hydrates - A promising source of energy. Journal of Natural Gas Science and Engineering 2010;2(1):49-59.

[10] Sun, C., Li, W., Yang, X., Li, F., Yuan, Q., Mu, L., Chen, J., Liu, B., Chen, G., Progress in Research of Gas Hydrate. Chinese Journal of Chemical Engineering 19, 2011, 151-162.

[11] Van der Waals J, Platteeuw J. Clathrate solutions. Advances in Chemical Physics, Volume 2 1959:1-57.

[12] Chen G-J, Guo T-M. Thermodynamic modeling of hydrate formation based on new concepts. Fluid Phase Equilibria 1996;122(1–2):43-65.

[13] Chen G-J, Guo T-M. A new approach to gas hydrate modelling. Chemical Engineering Journal 1998;71(2):145-151.

[14] Sun X, Mohanty KK. Kinetic simulation of methane hydrate formation and dissociation in porous media. Chemical Engineering Science 2006;61(11):3476-3495.

[15] Englezos P, Kalogerakis N, Dholabhai P, Bishnoi P. Kinetics of formation of methane and ethane gas hydrates. Chemical Engineering Science 1987;42(11):2647-2658.

[16] Kashchiev D, Firoozabadi A. Driving force for crystallization of gas hydrates. Journal of Crystal Growth 2002;241(1–2):220-230.

[17] Gnanendran N, Amin R. Modelling hydrate formation kinetics of a hydrate promoter–water–natural gas system in a semi-batch spray reactor. Chemical engineering science 2004;59(18):3849-3863.

[18] Ma QL, Chen GJ, Sun CY. Vapor–liquid–liquid–hydrate phase equilibrium calculation for multicomponent systems containing hydrogen. Fluid Phase Equilibria 2013;338(0):87-94.

[19] Ma Q, Chen G. Simulation of hydrate separation tower for water-in-oil emulsion system. CIESC Journal 2010;61(9):2401-2408.

[20] PetroChina Company Limited, Petroleum CUo, inventors; Google Patents, assignee. Combined process for separating and recovering hydrogen, ethylene and ethane from refinery dry gas or separating ethylene cracking gas2005 Dec 14, 2005.

[21] Badssi A, Bugarel R, Blanc C, Peytavy JL, Laurent A. Influence of pressure on the gas-liquid interfacial area and the gas-side mass transfer coefficient of a laboratory column equipped with cross-flow sieve trays. Chemical Engineering and Processing 1988;23(2):89-97.

[22] Sinnott R.K., Chemical engineering design: SI Edition: Elsevier; 2009.

[23] Peng DY, Robinson DB. A new two-constant equation of state. Industrial and Engineering Chemistry Fundamentals 1976;15(1):59-64.

[24] Anderson, G.K., 2003. Enthalpy of dissociation and hydration number of carbon dioxide hydrate from the Clapeyron equation. The Journal of Chemical Thermodynamics 35, 1171-1183.

[25] Ballard AL, Sloan Jr ED. Hydrate phase diagrams for methane + ethane + propane mixtures. Chemical Engineering Science 2001;56(24):6883-6895.

[26] Ma Q, Chen G, Zhang L. Vapor-hydrate phases equilibrium of $(CH_4+C_2H_6)$ and $(CH_4+C_2H_4)$ systems. Petroleum Science 2008;5(4):359-366.

Nomenclature:

Symbols	Unit	Description
Capital letters		
A		kinetic parameters for hydration
A'		Antoine constants for calculating standard fugacity
B'		Antoine constants for calculating standard fugacity
C'		Antoine constants for calculating standard fugacity
C		Langmuir constant
D	m	column diameter
H	J/s	heat
HG	mol/s	total gas consumption for hydrate formation per stage
HY	mol/s	total hydrate mole flow rate per stage
K		kinetic parameters for hydration
L	mol/s	total liquid mole flow rate per stage
N		the number of total stages
P	Pa	pressure
Q	J/s	total heat draw out per stage
R		ideal gas constant
R_e		Reynolds number
R_{ec}		Reynolds number for starting turbulence
SP	m^{-3}	slurry volume per stage
T	K	Temperature
V	mol/s	total vapour mole flow rate per stage
W	mol/s	total water mole flow rate per stage
X		Antoine constants for calculating the Langmuir constant
Y		Antoine constants for calculating the Langmuir constant
z		Antoine constants for calculating the Langmuir constant
Case letters		
c		the number of total components
h		flow weir of sieve plate internal
m	mol/mol	component mole fraction in hydrate phase
r	Kmol/min/ m^{-3}	hydrate generation rate per stage
Δt_j	min	slurry residence time per stage
x	mol/mol	component mole fraction in vapour phase
y	mol/mol	component mole fraction in liquid phase
z	mol/mol	component mole fraction in water phase
Latin		
$\Delta\mu$	J/s	driving force for hydration
θ		mole fraction in small cave
α		Constant
λ_1		the number of small cave in hydrate
λ_2		the number of large cave in hydrate
ρ	kg/ m^3	Density
Superscript		
^{f}		Flash
*		big cave in hydrate
Subscript		
abs		absorption process

DC	plate downcomer
hyd	hydration process
HY	hydrate phase
i	component i in the mixture; $i = 1, \dots, c$;
j	number j stage; $j = 1, \dots, N$
L	liquid phase
ow	outlet wire of plate
r	hydraulic head loss for resistance on plate
t	total hydraulic head loss on plate
V	vapour phase
W	water phase
0	standard conditions

Table 1

Column type selection for HHA process

Features of HHA	Plate column		Packed column	
	Adapt.	Explanation	Adapt.	Explanation
operating temperature is around 274.15K	√	metal material normally	√	plastic or metal material
operating pressure is around 3-5Mpa	√	a stable performance under high pressure	×	unstable liquid film under high pressure[21]
emulsion with hydrate solids content	√	good plug resistance [22]	×	easy to be plugged
long liquid residence time because of slow hydrate formation rate	√	appropriate plate structure design can achieve long residence time	×	low liquid hold-up and short residence time [22]
the heat generated inside column needs to be draw out	√	Cooling coils can be installed on the plates [22]	×	It is hard to install a cooling system inside a packing bed

Table 2

Parameters related with hydrate formation [19]

Component	Parameters of hydrate formation		Hydrate formation heat
	K (kmol/m^3/min)	A	(kJ/kmol)
CH_4	0.0902	-2.5200E+05	54200
CO_2	0.5060	-2.1830E+06	60700 [24]
C_2H_4	0.7425	2.7479E+08	70240
C_2H_6	0.0275	-1.9220E+06	71800
C_3H_8	0.0289	3.7135E+07	*

*: There is no data. The impact is neglected as the hydrate formation rate of this component is very small in this study.

Table 3

Parameters related with Chen-Guo method of each component [13, 18]

Gas	Antoine constant			SI structure			SII structure		
	X (bar)	Y (K)	Z (K)	A' (bar)	B' (K)	C'(K)	A' (bar)	B' (K)	C'(K)
H_2	5.64E-06	120.775	253.1	1.0000E+10	0.00	0.00	1.0000E+23	0.00	0.00
O_2	9.50E-06	2452.29	1.03	6.2498E+11	-5353.95	25.93	4.3195E+23	-12505.00	-0.35
N_2	4.32E-06	2472.37	0.64	9.7939E+11	-5286.59	31.65	6.8165E+23	-12770.00	-1.10
CH_4	2.30E-06	2752.29	23.01	1.5844E+13	-6591.43	27.04	5.2602E+23	-12955.00	4.08
CO^*									
CO_2	1.65E-06	2799.66	15.9	9.6372E+10	-6444.50	36.67	3.4474E+23	-12570.00	6.79
$C_2H_4^{**}$				4.8418E+11	-5597.59	51.80	3.7700E+21	-13841.00	0.55
$C_2H_6^{**}$				4.7500E+11	-5465.60	57.93	3.9900E+21	-11491.00	30.40
$C_3H_8^{**}$				1.0000E+12	-5400.00	55.50	4.1023E+23	-12312.00	39.00

*: There is no data for CO for Chen-Guo model and the data used in the model are same with CO_2.

**: For the blank, the value is assumed to zero in the calculation. The physical meaning is that the big molecules cannot occupy the small caves in hydrate.

Table 4

Hydrate structure parameters [13]

Structure	λ_1	λ_2	β (K/Pa)
SI	1/23	3/23	0.000004242
SII	2/17	1/17	0.000010224

Table 5

Stream results for HHA column

Item	Unit	Gas feed	Solvent feed	Gas out	Slurry out
Flowrate	Kmol/hr	387.381	387.381	321.2496	453.606
Temperature	K	274.15	274.15	274.15	274.15
Pressure	Mpa	3.1	3.05	3	3.01
composition					
H_2	mol%	20.65	-	24.63	0.19
O_2	mol%	0.39	-	0.44	0.02
N_2	mol%	24	-	28.19	0.5
CH_4	mol%	23.72	-	25.24	2.17
CO	mol%	0.61	-	0.27	0.51
CO_2	mol%	2.23	-	1.26	1.87
C_2H_4	mol%	20.54	-	15.29	7.03
C_2H_6	mol%	7.62	-	4.65	3.36
C_3H_8	mol%	0.24	-	0.02	0.2
$C_{10}H_{22}$	mol%	-	22.83	-	19.31
H_2O	mol%	-	77.17	-	64.85

Table 6

Column parameters

Item	Unit	Value
Number of stages		20
Diameter	m	0.8
Plate type		Sieve
Plate space	m	0.50
Liquid flow path		1
Weir height	m	0.08
Weir length/diameter ratio		0.85
Pressure of top plate	MPa	3
Temperature of top plate	K	274.15
flooding factor	%	73
Total pressure drop	MPa	0.0186

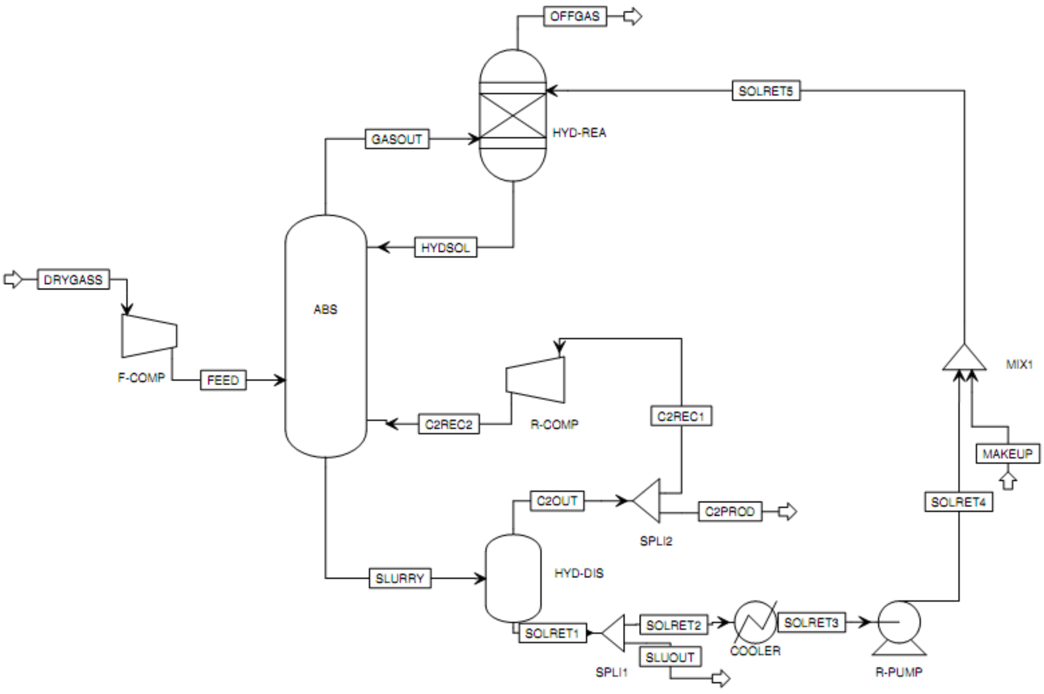

Fig.1. Schematic diagram of HHA process for ethylene recovery from refinery dry gas [8]. F-COMP , the gas feed compressor; ABS, the HHA column; HYD-REA, the hydration reactor; R-COMP, the gas recirculation compressor; HYD-DIS is the hydrate dissociation tank; COOLER, the cooler of solvent recycle; R-PUMP, the lean solvent pump.

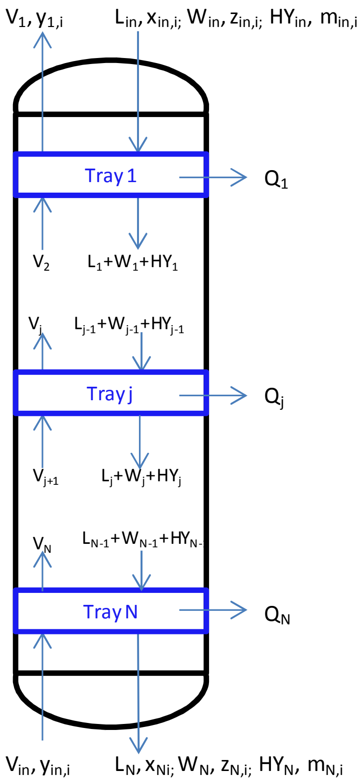

Fig.2. The sketch of multi-stage HHA column

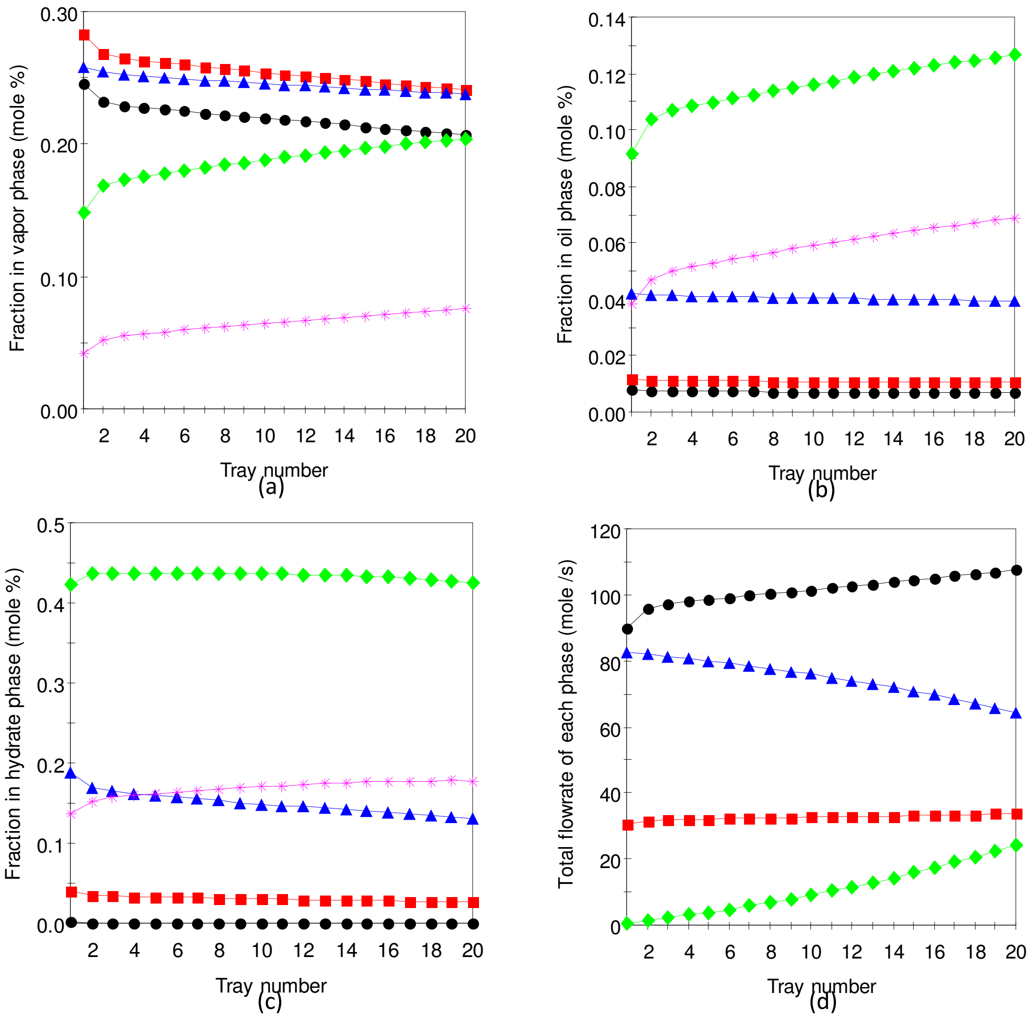

Fig.3. Composition distribution in each phase inside the column. For (a), (b) and (c), black dot (●), H_2; red box (■), N_2; blue triangle (▲), CH_4; green diamond (◆), C_2H_4; pink star (✳), C_2H_6; For (d), black dot (●), in vapor phase; red box (■), in oil phase; blue triangle(▲), in water; green diamond (◆), in hydrate phase.

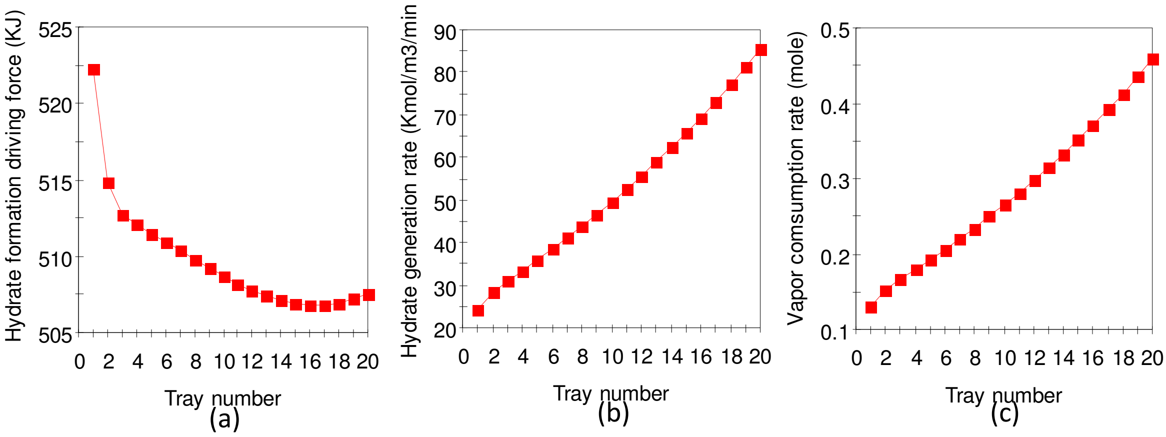

(a) (b) (c)

Fig.4. Parameters related with kinetic controlled hydrate formation

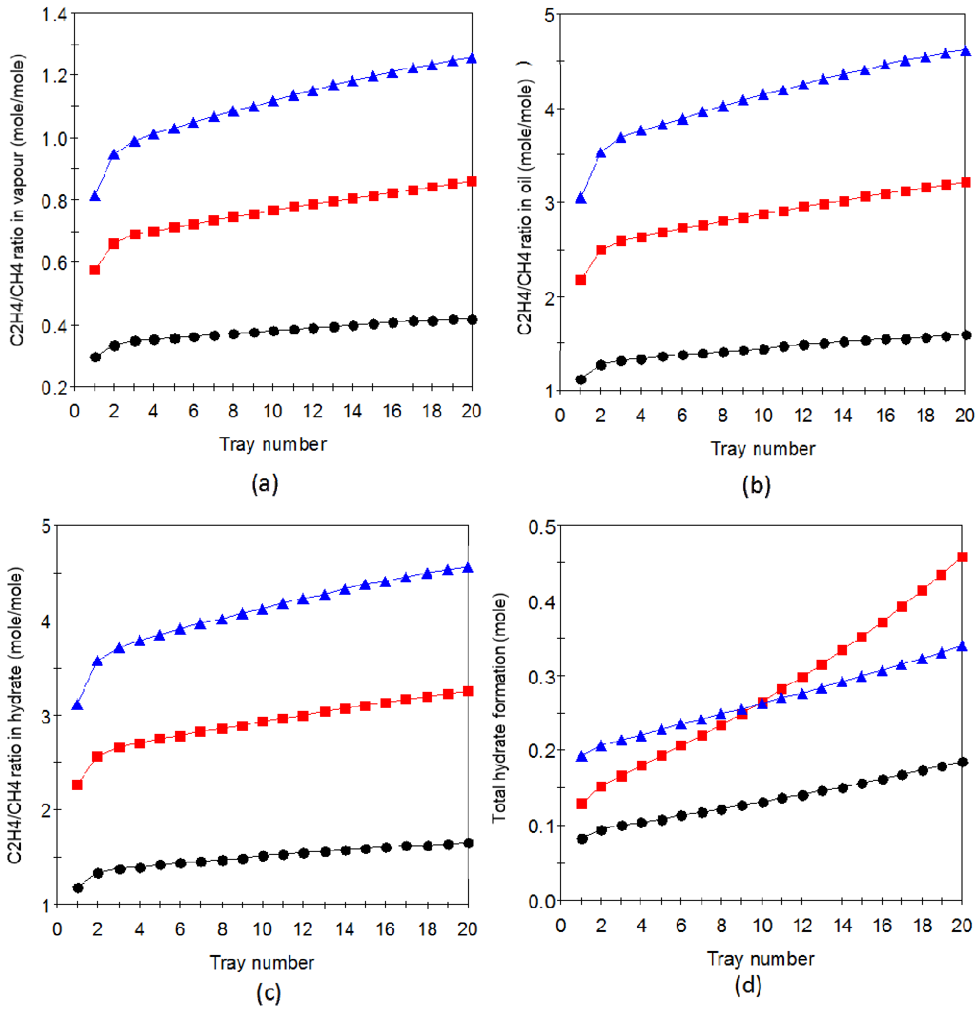

Fig.5. HHA column performance for different C_2H_4 concentrations in gas feed. For (a), (b), (c) and (d), black dot (●), 10 mole %; red box (■), 20.54 mole %; blue triangle (▲), 30 mole %.

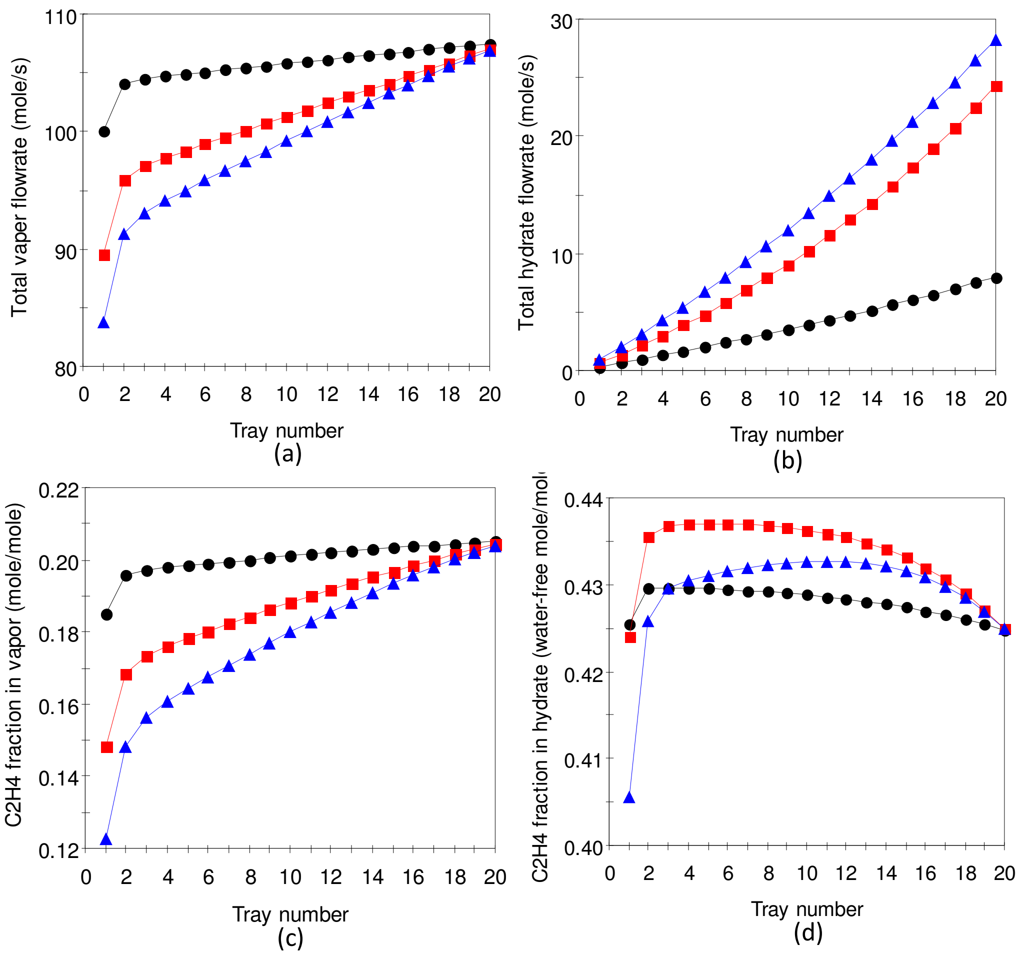

Fig.6. HHA column performance for different L/G ratios. For (a), (b), (c) and (d), black dot (●), L/G ratio of 0.5; red box (■), L/G ratio of 1.0; blue triangle (▲), L/G ratio of 1.5.

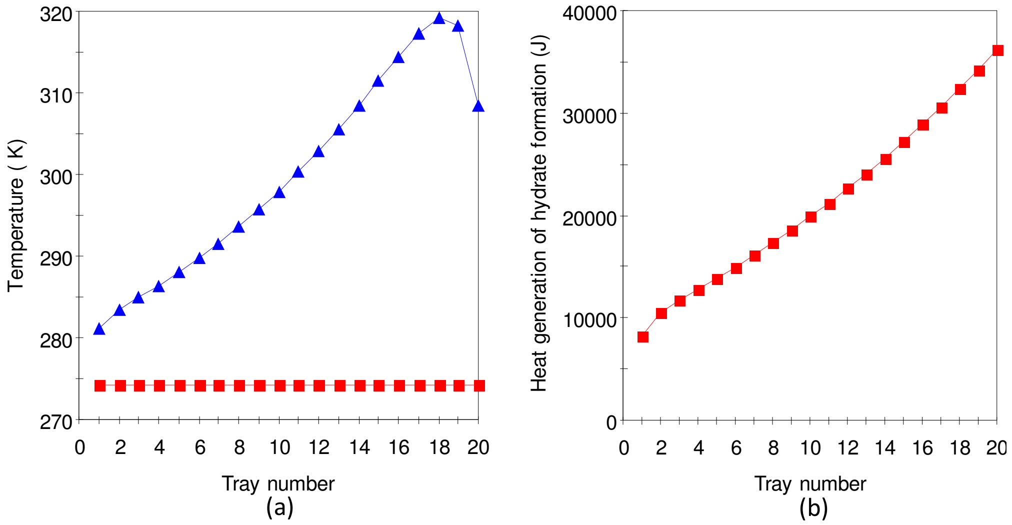

(a)

(b)

Fig.7. Temperature profile and heat generation of HHA process. For (a), red box (■), heat draw out case; blue triangle (▲), no heat exchange case.